

Study on Oscillation Starting Condition of K-Band Oversized Backward Wave Oscillator Driven by a Weakly Relativistic Electron Beam

OGURA Kazuo, YOSHIDA Ryo, YAMASHITA Yuichiro, YAMAZAKI Hosiyuki,
KOMIYAMA Kiyofumi and SAKAI Masakazu

Graduate School of Science and Technology, Niigata University, Niigata, 950-2181, Japan

(Received: 9 December 2003 / Accepted: 11 March 2004)

Abstract

Oscillation starting condition of a K-band oversized backward wave oscillator (BWO) is investigated experimentally. Periodically corrugated slow-wave structure (SWS) is used, which is designed for K-band operation in a weakly relativistic region, i.e. 30-80 kV. The beam current is in the range of 50-200 A. It is shown experimentally that there exists a critical beam energy (starting energy) for the meaningful radiation. The starting energy is more critical than the starting current in the oversized BWO. It decreases by increasing the SWS length. Above the starting energy, the output powers up to about 100 kW are obtained. The typical frequency observed is about 23 GHz. Nonaxisymmetric hybrid HE_{11} mode as well as axisymmetric TM_{01} mode is observed. The operation mode is able to be controlled by the SWS length and the magnetic field strength.

Keywords:

oversized backward wave oscillator, K-band, weakly relativistic electron beam, axisymmetric mode, nonaxisymmetric mode, starting energy

1. Introduction

Slow-wave high-power microwave devices such as backward wave oscillator (BWO) and traveling wave tube can be driven by an axially injected electron beam without initial perpendicular velocity and has been studied extensively as a candidate for a high power microwave source [1]. However, the radiation characteristics of the slow-wave device have been inferior in the frequency region above 10 GHz. In order to increase the frequency and/or the power handling capability, oversized slow-wave structures (SWSs) have been successfully used [2-6], in which diameter D of SWS is larger than free-space wavelength λ of output electromagnetic wave by several times or more. Among various oversized slow-wave devices, the multi-wave Cherenkov oscillator and the relativistic diffraction generator have attained record outputs of multi-GW levels at $\lambda = 30$ mm ($D/\lambda \approx 3$) and in the range of $\lambda = 9 - 11.3$ mm ($D/\lambda \approx 3$) [2]. These experiments are aimed at getting a GW-pulse of microwave using an intense relativistic electron beam above 1 MeV. A huge pulsed power supply is required. For practical applications and fundamental study, devices operating at reduced voltage are preferable [3-6].

It has been theoretically predicted that there exist two threshold conditions for the oscillation of BWO [7]. One is

the well-known starting current and has been studied for the conventional BWOs. The other is a starting energy and may become more critical than the starting current in the oversized BWO. Although this has been pointed out for the first time by the theoretical work in Ref. [7], there are few experimental studies on this subject. Further, in the oversized devices, the mode competition has been a serious problem.

In this work, a K-band oversized BWO is studied experimentally. Unique features of this BWO are (1) it is driven by a weakly relativistic electron beam less than 100 kV, (2) a relatively high beam current up to the range of 100 A can be used and (3) the operation frequency is in the range of 20 GHz. Note that the operation beyond 10 GHz is difficult for the conventional non-oversized slow-wave devices. It is shown experimentally that the starting energy actually exists and is more critical than the starting current in the oversized BWO. The experimental result of starting energy is discussed by comparing with the theoretical predictions. The oscillation modes are investigated and their control is demonstrated.

2. Dispersion characteristics and starting condition of K-band BWO

The periodic SWS used consists of modular sections

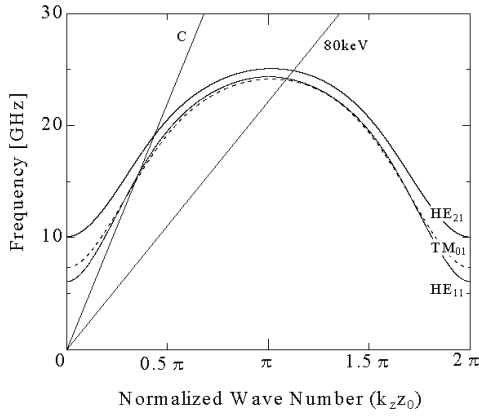


Fig. 1 Dispersion curves of HE_{11} , TM_{01} , and HE_{21} . As reference, lines of 80 keV beam and light are shown.

having a sinusoidally corrugated wall. Chosen parameters of the modular are as follows: average radius $R_0 = 15$ mm, corrugation amplitude $h = 1.7$ mm and pitch length $z_0 = 3.4$ mm. Each modular is fabricated from aluminum and includes ten corrugation periods. The radial boundary conditions at the wall connect the frequency f and the axial wave number k_z by the dispersion relation,

$$D(f, k_z) = 0. \quad (1)$$

Figure 1 shows the dispersion curves for the lowest three modes: an axisymmetric transverse magnetic (TM_{01}) and nonaxisymmetric hybrid (HE_{11} and HE_{21}) modes. Combinations of two letters of HE and EH are often used for the designation of hybrid mode. In this paper, the definition in the plasma physics is used, which is used in Refs. [8,9]. Note that this is opposite to the definition used in the field of corrugated waveguide [5,6]. The beam less than 100 keV will couple to the backward electromagnetic modes near the upper cutoffs in the frequency band of 20 GHz. The SWS is oversized with $D/\lambda \approx 2$. The total length L of SWS can be changed by changing the number of modular.

For a finite length BWO, the reflection at both ends leads to standing waves. In order to treat this effect, the axial boundary condition should be added. The beam interaction can be expressed by the following equations [7].

$$D(f, k_b) = 0 \quad (2)$$

$$D(f, k_z^-) = 0 \quad (3)$$

$$R_1 R_2 \exp\{-i(k_z^- - k_b)L\} = 1 \quad (4)$$

Here, k_z^- and k_b are respectively the wave number of backward electromagnetic and the beam mode, R_1 is the refraction coefficient at the beam entrance and R_2 is that at the other end. Equation (4) comes from the requirement that the field must be a single value at any axial position, after one round trip of the field. In the limit of infinite L , k_b and k_z^- coincide and form a saddle point, resulting in the oscillation due to an absolute instability. For finite L , however, the oscillation will

not occur at the saddle point.

For oscillations in the finite length BWO, two thresholds are imposed from the real and imaginary part of eq. (4). The imaginary part mainly determines the starting current. The real part is

$$\text{Re}(k_z^- - k_b) = 2\pi N/L. \quad (5)$$

Here, N is an integer corresponding to the spatial harmonic of the periodic system and $N = -1$ harmonic is dominant [7]. In order to satisfy eq. (5), the interaction width Δk_z in the wave number space should be larger than $2\pi/L$. In the oversized BWO, this condition becomes critical and cannot be satisfied by increasing only the beam current. The numerically obtained Δk_z for TM_{01} is shown in Fig. 2. By increasing beam energy, the interaction point approaches the π point in Fig. 1 and Δk_z increases as shown Fig. 2. At a critical beam energy (starting energy), Δk_z may become broad enough to satisfy eq. (5).

3. Experimental setup

Electron beam diode consists of a copper mesh anode and a hollow cold cathode with velvet on the edge. In the experiments, output voltage up to about 80 kV from the pulse-forming line is applied to the cathode. Uniform magnetic field B_0 for beam propagation is provided by using ten solenoid coils. The maximum value of B_0 is about 0.9 T.

The microwave output is picked up by a rectangular horn antenna located typically 800 mm away from the output window. After providing adequate amount of attenuation, the output power is detected by crystal detectors. For the frequency measurement, received signals are split into two branches by a multi-hole directional coupler. One consists of a short waveguide and forms a prompt signal. The other is a delay line typically 40 m long and forms a delayed signal. The microwave frequency is able to estimate from the delay time between two signals. In order to measure the radiation pattern, the horn antenna is swung horizontally in an equatorial plane around a pivot at the center of output window. Measured electric polarizations are horizontal (θ) and perpendicular (φ).

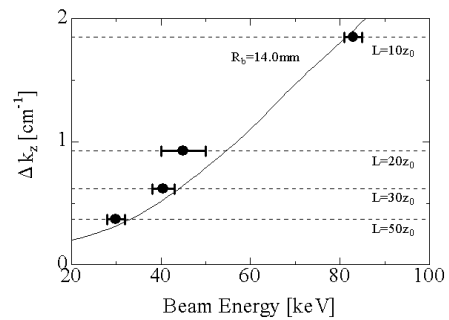


Fig. 2 Interaction width Δk_z versus beam energy. Experimentally obtained starting energies are also plotted.

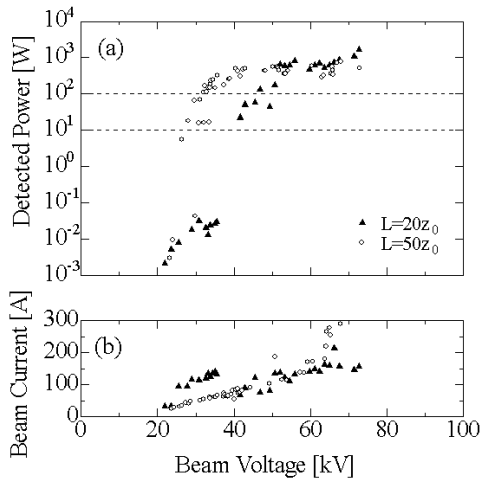


Fig. 3 (a) Detected power and (b) beam current versus beam voltage.

4. Experimental results

Figure 3 shows the detected microwave power and the beam current versus the beam voltage. In the experiment, the voltage and current change in time as shown in Fig. 4 and their values at time of microwave peak are used. By increasing the beam voltage, the abrupt increase of radiation is observed above about 40 kV and 60 A. The peak of current reaches up to about 100 A with voltage lower than 40 kV. Hence, the abrupt microwave increase in Fig. 3 cannot explain by the current and shows clearly the existence of the starting energy.

In the experiment, the starting energy is defined by the beam voltage, with which the power in the range of 10-100W is detected. The corresponding BWO output is estimated to be 0.5 – 5 kW. For $L = 20z_0$, the starting energy is 45 ± 5 keV. Above this, the output power increases gradually, due to the increase of input power. At 73 kV, the detected power is 2 kW, which corresponds to a BWO output of about 100 kW. For $L = 50z_0$, the starting energy decreases to 30 ± 3 keV. The starting energies for $L = 10z_0$ and $L = 40z_0$ are also measured and are summarized in Fig. 2. The starting energy shows a good coincidence to the theoretical prediction.

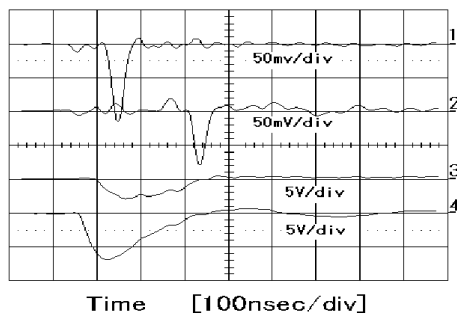


Fig. 4 Typical waveform of measured signals: 1 prompt signal, 2 delayed signal, 3 beam current and 4 beam voltage.

Figure 4 shows typical waveforms of microwave signal above the starting energy. The delay time between prompt and delayed signals is 181 nsec, which corresponds to the frequency of 23.4 GHz. This is close to the frequency of the crossing point between the 80 keV beam line and the fundamental TM_{01} or HE_{11} in Fig. 1.

In order to examine the mode, the radiation patterns of the oversized BWO are measured with about 50 kV, 200 A and 0.8 T. For $L = 20z_0$ (Fig. 5), the dominant mode of radiation is the axisymmetric TM_{01} . The TE_{01} component is also observed. The ratio of TE to TM is about 0.2 or less. For $L = 50z_0$ (Fig. 6), the radiation pattern is quite different from TM_{01} and can be explained by a rotating HE_{11} hybrid mode having the TE/TM ratio of one. Note that a peak at the center can be explained only by TE_{11} component. The peak is observed for both horizontal and perpendicular polarizations, and hence its electric polarization is rotating. The TM component can be detected only with the θ polarization.

In our experiment, the strength of the magnetic field B_0 also affects the oscillation mode. By changing B_0 from 0.8 T to 0.43 T, the mode changes from TM_{01} to HE_{11} . The mode change due to the SWS length and the magnetic field are interesting and important for practical devices.

5. Discussion and summary

The starting current is derived from the imaginary part of eq. (4), not the real part. The reflections at the ends of SWS should be considered properly. In the experiment, one

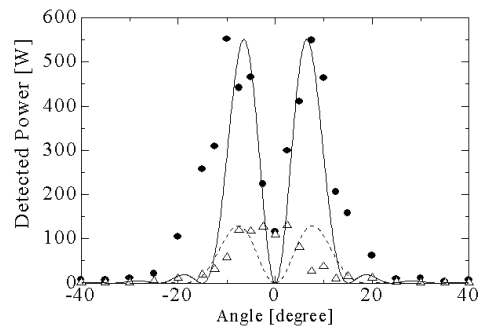


Fig. 5 Radiation patterns at $L = 20z_0$, with θ (●) and ϕ (△) polarization. Solid and dashed lines are theoretical curves for TM_{01} and TE_{01} modes, respectively.

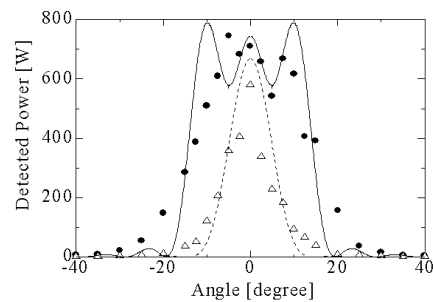


Fig. 6 Radiation patterns at $L = 50z_0$, with θ (●) and ϕ (△) polarization. Solid and dashed lines are theoretical curves for a rotating HE_{11} mode.

end of the SWS (beam entrance) is terminated to a mesh anode and the microwave may be reflected almost completely. At the other end, the SWS is “open” for the microwave extraction. Since the operation modes are near the π point, the group velocity of microwave is close to zero and the reflection at the open end may be large. The quality factor Q of the oversized SWS cavity may be comparable to the non-oversized SWS [5]. Hence, the starting current is expected to be less than 10 A [7]. This is consistent with the experimental result in Fig. 3.

The TM_{01} and HE_{11} modes are very close to each other as shown in Fig. 1. Nearly the same starting energy as TM_{01} is expected for the HE_{11} mode, because the interaction widths of two modes are of the same order [8]. They may be competing with each other. It is demonstrated that the mode is controlled by the strength of magnetic field and by the length of the SWS. The HE_{21} operation has not been confirmed in the experiment. This may be caused by the fact that the growth rate of HE_{21} is too small, about one tenth of that of TM_{01} and HE_{11} .

The TE components are observed even in the axisymmetric radiation. The normal modes of BWO driven by a magnetized electron beam become hybrid modes due to the anisotropy of magnetized electron [8,9]. For the axisymmetric mode, TE component is expected to be on the order of 1/10 of TM component. For nonaxisymmetric cases, the normal mode is hybrid due to the periodic wall. For HE_{11} , the TE/TM ratio is about one at the interaction point. The TE/TM ratios of the normal mode do not contradict the experimental results of Figs. 5 and 6.

The maximum power obtained is about 100 kW and the quality factor of microwave source is $Pf^2 \leq 6.0 \times 10^4$ [kW ·

GHz²]. This is much smaller compared with high-power microwave devices driven by a MV and kA beam. Our oversized BWO is aimed at “compact and easy to use” sources in the frequency range above 10 GHz, not at getting champion data. The mode control of the oversized BWO by the SWS length and the magnetic field is unique and of considerable interest for practical use.

Acknowledgements

This work was partially supported by a Grant-in-Aid for Scientific Research from the Ministry of Education, Science, Sports and Culture of Japan. Support of numerical calculations was afforded by the Computer Center, National Institute for Fusion Science.

References

- [1] J. Benford and J. Swegle, *High-Power Microwaves* (Artech House, Norwood, MA, 1992).
- [2] S.P. Bugaev *et al.*, IEEE Trans. Plasma Sci. **18**, 518 and 525 (1990).
- [3] Md.R. Amin *et al.*, J. Phys. Soc. Jpn. **64**, 4473 (1995).
- [4] K. Ogura *et al.*, Phys. Rev. E **53**, 2726 (1996).
- [5] A.N. Vlasov *et al.*, IEEE Trans. Plasma Sci. **28**, 550 (2000).
- [6] K. Ogura *et al.*, *Joint Technical Meeting on Plasma Science and Technology and Pulsed Power Technology*, (PST-02-67/PPT-02-24, Hawaii, USA 2002).
- [7] K. Minami *et al.*, IEEE Trans. Plasma Sci. **23**, 124 (1995).
- [8] O. Watanabe and K. Ogura, J. Plasma Fusion Res. SERIES **3**, 601 (2000).
- [9] O. Watanabe *et al.*, Phys. Rev. E **63**, 6503 (2001).